ACS Photonics
Letter
Cite This: ACS Photonics 2018, 5, 2742−2747

Lateral Heterogeneous Integration of Quantum Cascade Lasers

Yang Yang,*,† Andrew Paulsen,† David Burghoff,† John L. Reno,‡ and Qing Hu†

†Department of Electrical Engineering and Computer Science, Research Laboratory of Electronics, Massachusetts Institute of Technology, Cambridge, Massachusetts 02139, United States

‡Center for Integrated Nanotechnology, Sandia National Laboratories, Albuquerque, New Mexico 87123, United States

Supporting Information

ABSTRACT: Broadband terahertz radiation potentially has extensive applications, ranging from personal health care to industrial quality control and security screening. While traditional methods for broadband terahertz generation rely on bulky and expensive mode-locked lasers, frequency combs based on quantum cascade lasers (QCLs) can provide an alternative compact, high power, wideband terahertz source. QCL frequency combs incorporating a heterogeneous gain medium design can obtain even greater spectral range by having multiple lasing transitions at different frequencies. However, despite their greater spectral coverage, the comparatively low gain from such gain media lowers the maximum operating temperature and power. Lateral heterogeneous integration offers the ability to cover an extensive spectral range while maintaining the competitive performance offered from each homogeneous gain media. Here, we present the first lateral heterogeneous design for broadband terahertz generation: by combining two different homogeneous gain media, we have achieved a two-color frequency comb spaced by 1.5 THz.

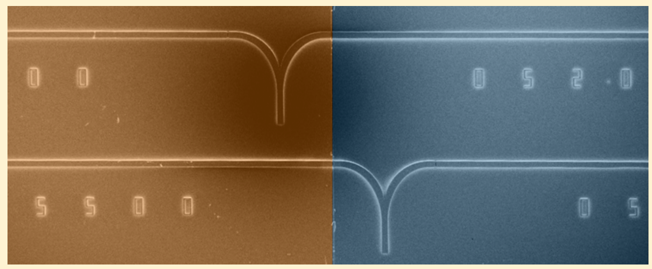

KEYWORDS: *semiconductor lasers, frequency combs, terahertz, monolithic integration, broadband sources*

The terahertz frequency regime has long attracted interest since many complex molecules have their absorption "fingerprint" within this energy range. For this reason, broadband terahertz measurements such as THz time-domain spectroscopy have been adopted both in the laboratory[1,2] as well as on production lines.[3] In the time-domain method, broadband terahertz radiation is generated via photoconductive switching or optical rectification, which requires an expensive mode-locked laser and often bulky optics. In contrast, QCL frequency combs offer high output power in a compact footprint and show strong potential as a useful tool for terahertz laser spectroscopy.[4,5] With great design versatility, one can engineer the gain media to lase at different frequencies within the same material system. Using this design versatility, separate gain media with various lasing frequencies can be carefully stacked together to form a heterogeneous gain medium.

The heterogeneous gain medium, first realized in the mid-infrared[6] and more recently in the THz,[7] has made significant progress in achieving broadband lasing. Excellent results have been reported using it to realize frequency combs[8] or to generate short terahertz pulses.[9] Despite these successes, the compromises inherent in heterogeneous gain media produce lower peak gain which hamper the laser's temperature and power performance. This can be especially problematic in the THz regime, where achieving gain above cryogenic temperature remains a challenging task. The result of the design trade-offs between spectral coverage and laser performance can be seen directly in devices made from a three-stack heterogeneous gain medium which lase up to 55 K under continuous-wave biasing,[8] while this temperature drops to 30 K for a four-stack medium.[10]

Here, we show that by using lateral integration, the trade-offs between temperature performance and spectral coverage can be eliminated. Lateral heterogeneous integration combines light from different gain media using a monolithically fabricated broadband light combiner. The performance of the individual gain media are preserved, while the overall device still covers an extensive large spectral range. This enables a new design scheme for the quantum cascade laser platform, while still maintaining a compact package. We present our first lateral heterogeneous design for broadband terahertz generation, and by combining two different gain media, we have already achieved a two-color frequency comb operation over a span of 1.5 THz, from 3.2 THz to 4.7 THz.

RESULTS

Design of the Broadband Terahertz Light Combiner. A key benefit from monolithic integration is its simplicity and compactness. For this reason, a terahertz light combiner is designed under the metal−metal waveguide geometry. Furthermore, by fully leveraging the high confinement from such waveguides, the actual device resembles a Y-branch with 90° half angle for compactness.[11] Figure 1a shows the schematic of our design. Modeled as a three-port system, we

Received: April 18, 2018
Published: June 7, 2018

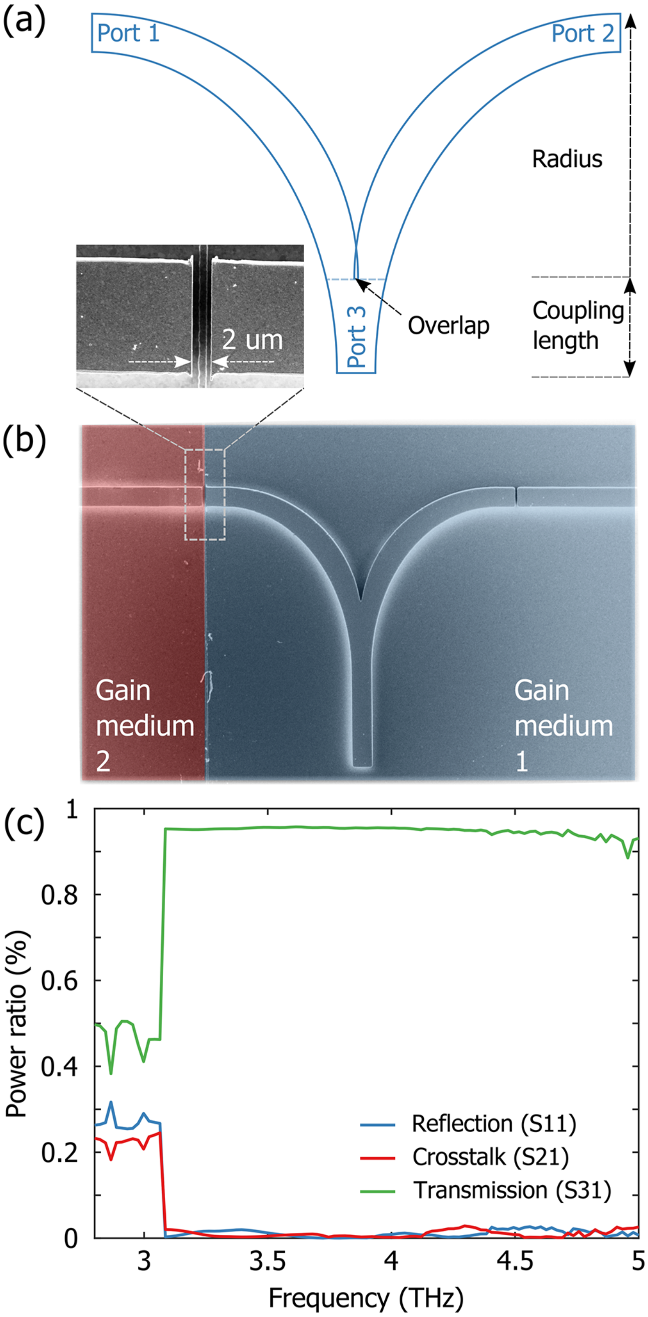

Figure 1. (a) Schematic of the combiner design. The outer radius, overlap between input ports, and coupling length are optimized to maximize the transmission and minimize reflection and crosstalk. (b) SEM images of the fabricated device. Pseudocolor is in use to distinguish original gain media. The inset shows one of the 2 μm wide air gaps at the interface of the two gain media. (c) Simulated scattering parameters from the optimized combiner.

have fixed the width of ports and the height of the combiner to be the same as devices to be integrated (in this case, the width of the ports is 20 μm and the height is 10 μm). In order to design such a combiner that maximizes the transmission while minimizing crosstalk and reflection over a broad spectral range, a genetic algorithm is used to optimize the combiner's design. Three critical parameters, namely, the outer bending radius, the overlap distance between two input ports, and the coupling length, are fed into the optimizer. The only free parameter left, the inner bending radius, is automatically adjusted to make an adiabatic transition. (All optimization details can be found in the Methods section.) The optimized design possesses an outer bending radius of 139 μm, an overlap distance of 2 μm, and a coupling length of 49 μm. The simulated scattering parameters from the optimized combiner are presented in Figure 1c. Over the range 3.1−5 THz, the combiner maintains a power transmission ratio greater than 95% with negligible reflection and crosstalk.

Monolithic Integration for Broadband Spectral Coverage. Two resonant-phonon gain media are chosen for their spectral coverage and good temperature performance: Gain Medium 1 spans from 3.2 to 3.8 THz and it lases up to 144 K,[12,13] while Gain Medium 2 covers 3.9 to 4.8 THz and it lases up to 153 K.[14] Laser devices made from both gain media also are well-characterized in terms of dispersion and frequency comb operation capabilities in previous projects.

To realize the monolithic integration, two different gain-medium pieces are sequentially bonded and aligned to the same receptor wafer. By joining the gain-medium pieces along their cleaved crystal facets, the clearance between two pieces can be less than 1 μm (see Supporting Information for more information). Figure 1b depicts the actual fabricated device. In the present case, the combiner is defined on Gain Medium 1. The pseudocolor is used to illustrate the two different gain media, from which two laser devices with their own dispersion compensators on the rear end (not shown) are monolithically integrated to the combiner's input ports. Two 2 μm wide air gaps separate the combiner from laser devices to enable their independent biasing controls and satisfactory coupling efficiency.[13] The lengths of the laser device on Gain Medium 1 (Laser 1) and Gain Medium 2 (Laser 2) are roughly 2.14 and 2 mm separately. The details for dispersion compensators of these two lasers can be found in the Methods section, both of whose parameters are adapted from previous projects for proper frequency comb operation.

Light-Current Characteristics of the Device. Since the combiner is made from one laser gain medium (in this case, Gain Medium 1), we have investigated the influence of biasing the combiner on the output power at 25 K. Note that the combiner achieves lasing above 80 mA, so in all the following characterization, the combiner's biasing is kept below 80 mA (see Supporting Information for more information about the combiner characterization). Figure 2a shows the light-current relations for lasers at different input ports when the combiner is off or biased at a subthreshold value. The jagged light-current characteristics primarily reflect the broadband lasing nature of such device, which we have observed in the past.[13] As we increase the combiner's biasing, Laser 2 shows a steady overall increase in output power, while the output power from Laser 1 remains approximately constant. The average output power from the two devices is plotted in Figure 2b, normalized to the power collected from their unbiased-combiner state. It is evident that, for better power performance, biasing the combiner to a subthreshold value is preferable. Note that for Laser 1, the combiner shows moderate absorption at its lasing frequencies before biased above 70 mA (for example, the "dip" at ~50 mA), which is consistent with gain characterization results from gain media of similar designs.[15] For Laser 2, the increasing output power actually results from a reduction in losses due to intra-injector absorption in Gain Medium 1: when unbiased, the absorption between the ground and first excited state in the injector wells is at around 4 THz with an oscillator strength of 0.26. As the biasing on the combiner is turned up,

DOI: 10.1021/acsphotonics.8b00507
ACS Photonics 2018, 5, 2742−2747

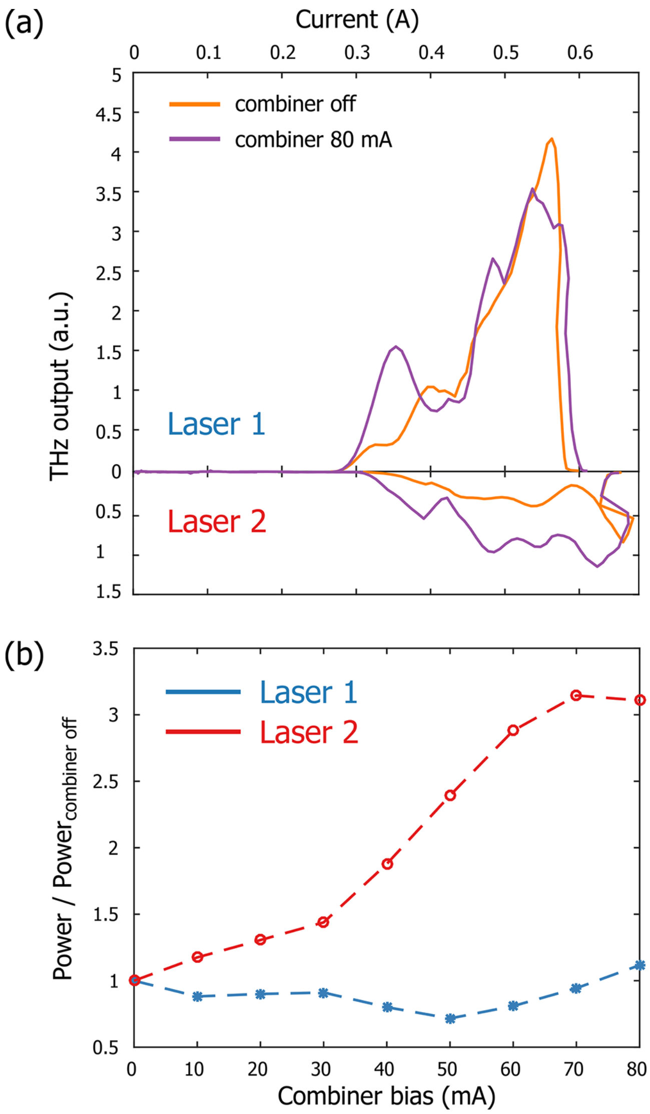

Figure 2. (a) Light-current characterization for both lasers under different combiner biasing points. (b) Average power from both lasers. The average power is showing in ratio using the power collected from their unbiased-combiner state as a reference.

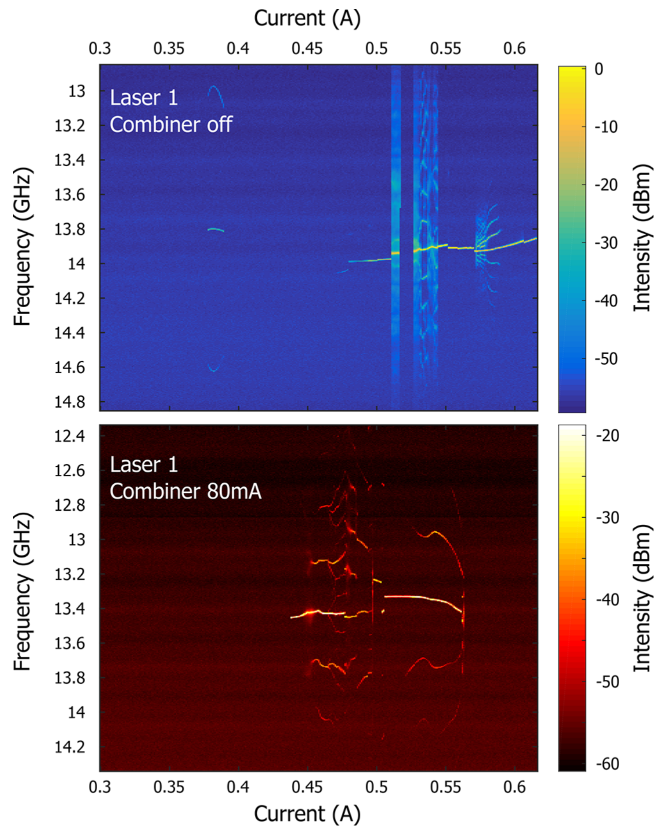

Figure 3. Microwave-frequency maps for Laser 1's repetition rate characterization. The top panel shows the repetition rate map when combiner is unbiased, and the bottom panel shows the repetition rate map when combiner is biased to 80 mA.

electrons empty out the ground state and flow into the first excited state, causing a rapid decrease of its high-frequency absorption. Since the combiner is never biased above its lasing threshold, the section is moderately lossy and the Gires-Tournois-like interference due to the air gap is consequently eliminated. Lateral heterogeneous devices with combiner on Gain Medium 2 are also fabricated and characterized; more details about their measurement results can be found in the Supporting Information.

Two Color Frequency Combs. One unique property for QCL frequency combs is that when they are biased under continuous-wave conditions, devices generate a strong microwave-frequency intermode beating signal at their repetition-rate frequency. This single and strong repetition-rate beatnote signal is a telltale sign of comb operation for such devices.[4,5,8,10]

We have investigated the microwave-frequency spectra around lasers' repetition rate frequencies and also evaluated the influence from combiner's biasing on the microwave-frequency characteristics of the integrated lasers. Figures 3 and 4 present the repetition-rate maps from individual lasers, both when combiner is unbiased and when it is biased to the subthreshold value. Due to length and refractive index differences, Laser 1 has a repetition rate around 14 GHz, while Laser 2's repetition rate is about 15 GHz. Similar to the case where the lasers are separated, both lasers possess different modes of behavior such as single beatnote, multiple beatnotes, and broad beatnote regimes within their biasing range.[13] From Figure 3 it is also apparent that when the combiner's biasing increases to 80 mA, the repetition rate for Laser 1 decreases from 14 to 13.4 GHz. The repetition rate's frequency change for Laser 2 is not significant with changes in combiner's biasing. Although the higher bias on the combiner does favor more robust comb operation for Laser 2, showing a strong single repetition rate beatnote, as shown in Figure 4. One explanation of how the biasing of the combiner influences the repetition rate behaviors of the lasers is that it essentially introduces a dynamic change of the absorption and dispersion relation to the lasers, suggesting a strong coupling between the combiner and the laser devices.

One critical thing to note is that irrespective of the combiner's biasing, frequency comb operation from both lasers with different repetition rate frequencies, two-color frequency combs, can be obtained. Figure 5 shows the terahertz spectra collected from the output port of the combiner as well as their corresponding microwave-frequency spectra under two biasing conditions. The integrated device possesses a spectral coverage of 1.5 THz (not continuous) ranging from 3.2 to 4.7 THz and with more than 50 laser lines. Similar measurement results from the integrated device whose combiner is on Gain Medium 2

DOI: 10.1021/acsphotonics.8b00507
ACS Photonics 2018, 5, 2742−2747

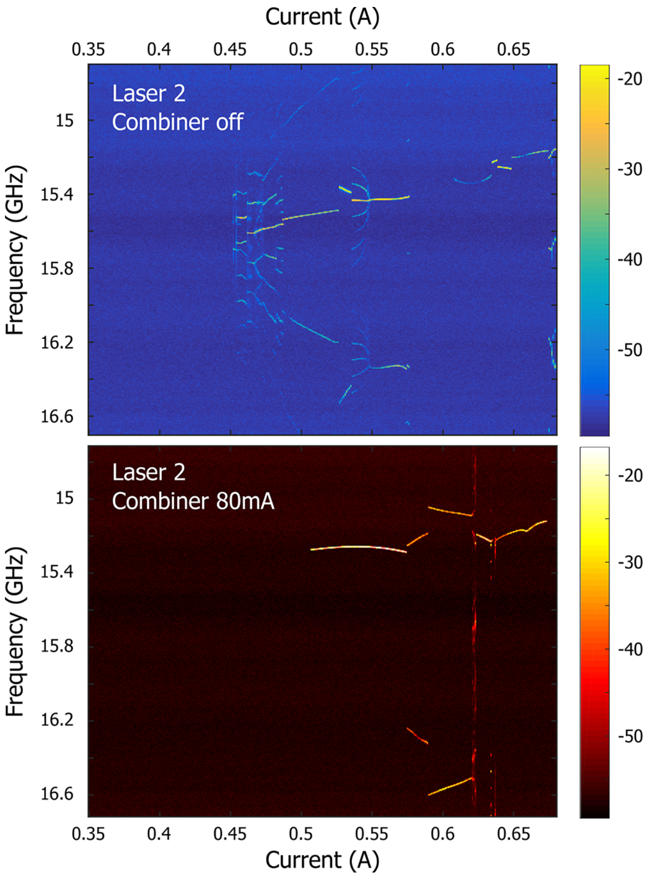

Figure 4. Microwave-frequency maps for Laser 2's repetition rate characterization. The top panel shows the repetition rate map when combiner is unbiased, and the bottom panel shows the repetition rate map when combiner is biased to 80 mA.

can be found in the Supporting Information. One thing to note is that the maximum temperature for the integrated device under continuous-wave operation is determined by Laser 1, which lases up to 75 K (Laser 2 continues lasing up to 89 K). Under pulsed bias operation, the corresponding number for Laser 1 is 110.5 K and 137 K for Laser 2. Given the fabrication and measurement variations, all of the measured temperature values match up with the reported results.[12−14]

■ CONCLUSIONS

In conclusion, we have demonstrated the lateral heterogeneous integration of quantum cascade lasers. In this work we have shown that such a scheme can be used for broadband terahertz generation. Our first laterally integrated devices cover a frequency range of almost 1.5 THz with more than 50 laser lines by only incorporating two different gain media. Similar techniques can be used to improve the spectral coverage, even at other wavelength bands, including the mid-infrared.[16,17] We have clearly demonstrated a two-color frequency comb operating from 3.2 to 4.7 THz; further development in dispersion engineering of the laser devices could lead to a continuous coverage across this range. To explore an octave-spanning frequency comb operation capable of f-2f locking may require the use of additional gain media, which can be easily implemented using the general design approach presented in this paper. The combiner may be an ideal port to extract the f-2f beating signal through the intracavity mixing process.[4] The different repetition rates from the two (or more) lasers will introduce some complexity in the actual spectral data analysis. Fortunately, this issue is straightforward to resolve as we properly calibrate the relationship between laser length and repetition rate; integrated lasers with similar repetition rates may be able to achieve repetition rate frequency locking via mutual microwave-frequency pulling or via external microwave-frequency injection locking.[18] Furthermore, this lateral heterogeneous integration scheme itself has broader applications in device development. As a platform it can be adapted to solve challenges such as passive mode locking using multi-section QCLs[19] or distributed feedback laser arrays for broadband coverage.[20] It could also be used for novel lab-on-a-chip system designs, such as monolithically integrated spectrometers[21] and transceivers[22] in the long-wavelength regime. Our lateral heterogeneous integration can eliminate the design trade-offs in so-called bifunctional gain media,[23] allowing more freedom to integrate quantum-structure sources and detectors.

■ METHODS

Optimization for Broadband Terahertz Light Combiner Design. Scattering parameters can be found using 3D FEM simulations from which we can estimate the transmission, reflection, and crosstalk of the simulated

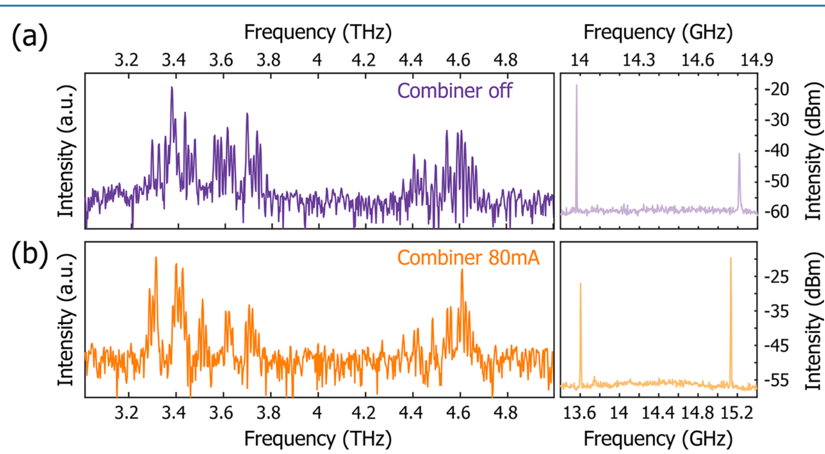

Figure 5. Terahertz spectra and microwave-frequency spectra under various biasing conditions. (a) Biasing on Laser 1 is 0.4835 A and on Laser 2 is 0.6625A. The combiner is unbiased. (b) Biasing on Laser 1 is 0.4835 A and on Laser 2 is 0.655 A. The combiner is biased to 80 mA.

DOI: 10.1021/acsphotonics.8b00507
ACS Photonics 2018, 5, 2742−2747

Table 1. Parameters for the Dispersion Compensators

	length (μm)	starting period (μm)	starting phase	starting width (μm)	stop period (μm)	ending phase	stop width (μm)	width chirping parameter	sinusoidal power
Laser 1	336	8.4	0	20	15.58	π	3	1	2
Laser 2	361	7	0	20	12	π	3	1.2	2

structure. Two supported transverse modes of the waveguide are taken into consideration in the simulation, but only the fundamental mode is excited at the input port. No metal losses and material losses are taken into account when performing the scattering parameter simulations. Also, the simulation environment was surrounded with a perfect-matching layer to absorb unphysical reflections from the boundaries. The simulations were carried out using *COMSOL Multiphysics*, and the genetic algorithm was applied using *MATLAB*.

Dispersion Compensator Designs for Quantum Cascade Lasers. Double-chirped sinusoidal structures are used to design the dispersion compensators for both lasers.[4,13] The design parameters are tailored for each laser based on its emission frequency, group velocity dispersion, and its laser length. The key parameters used for dispersion compensators in this work are listed in the following Table 1. Among all of the parameters, the power of the sinusoidal function shapes the compensator's general appearance. The sinusoidal period linearly chirps from the start to the stop period, effectively governing the compensator's functional frequency range. Simultaneously, the width of the compensator is gradually chirped, the speed of the chirp is determined by the width chirping parameter. The goal for such a double-chirping strategy is to introduce a proper amount of opposite group dispersion delay to the laser device without suffering Gires-Tournois-like interference.

Repetition Rate Mapping. Repetition rate is electrically measured from the AC port of the bias tee that is used to bias the laser. To create a repetition rate map, spectra around the laser's repetition rate frequency are sequentially collected using a radio frequency spectrum analyzer. Pseudocolor is used to present the intensity in all repetition rate maps.

■ ASSOCIATED CONTENT

Supporting Information

The Supporting Information is available free of charge. The Supporting Information is available free of charge on the ACS Publications website at DOI: 10.1021/acsphotonics.8b00507.

Collection of additional data and methods that supports the main conclusions in the paper (PDF).

■ AUTHOR INFORMATION

Corresponding Author

*E-mail: yang_y@mit.edu.

ORCID

Yang Yang: 0000-0001-5715-2206

Notes

The authors declare no competing financial interest.

■ ACKNOWLEDGMENTS

The work was supported by the NSF, the Defense Advanced Research Projects Agency (DARPA), and the U.S. Army Aviation and Missile Research, Development, and Engineering Center (AMRDEC) through Grant No. W31P4Q-16-1-0001. The views and conclusions contained in this document are those of the authors and should not be interpreted as representing the official policies, either expressed or implied, of the Defense Advanced Research Projects Agency, the U.S. Army, or the U.S. Government. This work was performed, in part, at the Center for Integrated Nanotechnologies, an Office of Science User Facility operated for the U.S. Department of Energy (DOE) Office of Science. Sandia National Laboratories is a multimission laboratory managed and operated by National Technology and Engineering Solutions of Sandia, LLC., a wholly owned subsidiary of Honeywell International, Inc., for the U.S. Department of Energy's National Nuclear Security Administration under Contract DE-NA-0003525. D.B. was supported by the Intelligence Community Postdoctoral Research Fellowship Program at MIT, administered by Oak Ridge Institute for Science and Education through an interagency agreement between the U.S. DOE and the Office of the Director of National Intelligence. Y.Y. also acknowledges the assistance of Ali Khalatpour for the fabrication process development.

■ REFERENCES

(1) Mittleman, D. M.; Hunsche, S.; Boivin, L.; Nuss, M. C. T-ray tomography. *Opt. Lett.* **1997**, *22*, 904−906.

(2) Fischer, B.; Hoffmann, M.; Helm, H.; Modjesch, G.; Jepsen, P. U. Chemical recognition in terahertz time-domain spectroscopy and imaging. *Semicond. Sci. Technol.* **2005**, *20*, S246.

(3) Wallace, V.; Fitzgerald, A.; Shankar, S.; Flanagan, N.; Pye, R.; Cluff, J.; Arnone, D. Terahertz pulsed imaging of basal cell carcinoma ex vivo and in vivo. *Br. J. Dermatol.* **2004**, *151*, 424−432.

(4) Burghoff, D.; Kao, T.-Y.; Han, N.; Chan, C. W. I.; Cai, X.; Yang, Y.; Hayton, D. J.; Gao, J.-R.; Reno, J. L.; Hu, Q. Terahertz laser frequency combs. *Nat. Photonics* **2014**, *8*, 462−467.

(5) Yang, Y.; Burghoff, D.; Hayton, D. J.; Gao, J.-R.; Reno, J. L.; Hu, Q. Terahertz multiheterodyne spectroscopy using laser frequency combs. *Optica* **2016**, *3*, 499−502.

(6) Gmachl, C.; Sivco, D. L.; Colombelli, R.; Capasso, F.; Cho, A. Y. Ultra-broadband semiconductor laser. *Nature* **2002**, *415*, 883−887.

(7) Dana, T.; Scalari, G.; Castellano, F.; Amanti, M. I.; Beck, M.; Faist, J. Ultra-broadband heterogeneous quantum cascade laser emitting from 2.2 to 3.2 THz. *Appl. Phys. Lett.* **2011**, *99*, 191104.

(8) Rosch, M.; Scalari, G.; Beck, M.; Faist, J. Octave-spanning semiconductor laser. *Nat. Photonics* **2015**, *9*, 42−47.

(9) Bachmann, D.; Rosch, M.; Suess, M. J.; Beck, M.; Unterrainer, K.; Darmo, J.; Faist, J.; Scalari, G. Short pulse generation and mode control of broadband terahertz quantum cascade lasers. *Optica* **2016**, *3*, 1087−1094.

(10) Rosch, M.; Beck, M.; Suess, M. J.; Bachmann, D.; Unterrainer, K.; Faist, J.; Scalari, G. Heterogeneous terahertz quantum cascade lasers exceeding 1.9 THz spectral bandwidth and featuring dual comb operation. *Nanophotonics* **2018**, *7*, 237−242.

(11) Manolatou, C.; Johnson, S. G.; Fan, S.; Villeneuve, P. R.; Haus, H. A.; Joannopoulos, J. D. High-Density Integrated Optics. *J. Lightwave Technol.* **1999**, *17*, 1682.

(12) Burghoff, D.; Yang, Y.; Reno, J. L.; Hu, Q. Dispersion dynamics of quantum cascade lasers. *Optica* **2016**, *3*, 1362−1365.

(13) Yang, Y.; Burghoff, D.; Reno, J.; Hu, Q. Achieving comb formation over the entire lasing range of quantum cascade lasers. *Opt. Lett.* **2017**, *42*, 3888−3891.

(14) Chan, C. W. I. Towards room-temperature Terahertz Quantum Cascade Lasers: directions and design. *Thesis*; Massachusetts Institute of Technology, 2015.

(15) Burghoff, D.; Kao, T.-Y.; Ban, D.; Lee, A. W. M.; Hu, Q.; Reno, J. A terahertz pulse emitter monolithically integrated with a quantum cascade laser. *Appl. Phys. Lett.* **2011**, *98*, 061112.

(16) Zhou, W.; Bandyopadhyay, N.; Wu, D.; McClintock, R.; Razeghi, M. Monolithically, widely tunable quantum cascade lasers based on a heterogeneous active region design. *Sci. Rep.* **2016**, *6*, 25213.

(17) Spott, A.; Stanton, E. J.; Volet, N.; Peters, J. D.; Meyer, J. R.; Bowers, J. E. Heterogeneous integration for mid-infrared silicon photonics. *IEEE J. Sel. Top. Quantum Electron.* **2017**, *23*, 1−10.

(18) Gellie, P.; Barbieri, S.; Lampin, J.-F.; Filloux, P.; Manquest, C.; Sirtori, C.; Sagnes, I.; Khanna, S. P.; Linfield, E. H.; Davies, A. G.; Beere, H.; Ritchie, D. Injection-locking of terahertz quantum cascade lasers up to 35 GHz using RF amplitude modulation. *Opt. Express* **2010**, *18*, 20799−20816.

(19) Tzenov, P.; Babushkin, I.; Arkhipov, R.; Arkhipov, M.; Rosanov, N.; Morgner, U.; Jirauschek, C. Passive and hybrid mode locking in multi-section terahertz quantum cascade lasers. *New J. Phys.* **2018**, *20*, 053055.

(20) Kao, T.-Y. From high power terahertz quantum cascade lasers to terahertz light amplifiers. *Thesis*; Massachusetts Institute of Technology, 2014.

(21) Schwarz, B.; Reininger, P.; Ristanic, D.; Detz, H.; Andrews, A. M.; Schrenk, W.; Strasser, G. Monolithically integrated mid-infrared lab-on-a-chip using plasmonics and quantum cascade structures. *Nat. Commun.* **2014**, *5*, 4085.

(22) Wanke, M. C.; Young, E. W.; Nordquist, C. D.; Cich, M. J.; Grine, A. D.; Fuller, C. T.; Reno, J. L.; Lee, M. Monolithically integrated solid-state terahertz transceivers. *Nat. Photonics* **2010**, *4*, 565−569.

(23) Schwarz, B.; Reininger, P.; Detz, H.; Zederbauer, T.; MaxwellAndrews, A.; Kalchmair, S.; Schrenk, W.; Baumgartner, O.; Kosina, H.; Strasser, G. A bi-functional quantum cascade device for same-frequency lasing and detection. *Appl. Phys. Lett.* **2012**, *101*, 191109.

DOI: 10.1021/acsphotonics.8b00507
ACS Photonics 2018, 5, 2742−2747